Electron delocalization of tensily strained GaAs quantum dots in GaSb matrix

T. C. Lin, Y. H. Wu, L. C. Li, Y. T. Sung, S. D. Lin, L. Chang, Y. W. Suen, and C. P. Lee

Citation: Journal of Applied Physics **108**, 123503 (2010); doi: 10.1063/1.3520669
View online: http://dx.doi.org/10.1063/1.3520669
View Table of Contents: http://scitation.aip.org/content/aip/journal/jap/108/12?ver=pdfcov
Published by the AIP Publishing

Electron delocalization of tensily strained GaAs quantum dots in GaSb matrix

T. C. Lin,[1,a)] Y. H. Wu,[2] L. C. Li,[3] Y. T. Sung,[4] S. D. Lin,[1] L. Chang,[2] Y. W. Suen,[4,5] and C. P. Lee[1,3]

[1]*Department of Electronics Engineering and Institute of Electronics, National Chiao Tung University, Taiwan*
[2]*Department of Materials Science and Engineering, National Chiao Tung University, Taiwan*
[3]*Center for Nano Science and Technology, National Chiao Tung University, Taiwan*
[4]*National Nano Device Laboratories, Taiwan*
[5]*Department of Physics and Institute of Nanoscience, National Chung Hsing University, Taichung, Taiwan*

(Received 12 July 2010; accepted 28 October 2010; published online 16 December 2010)

The magneto-optical response of type-II tensily strained GaAs self-assembled quantum dots in GaSb was investigated in magnetic fields up to 14 T. By depositing different GaAs amount, the dot sizes and the corresponding emission energies were varied. We analyzed the carrier wave function extent of different dots using the diamagnetic shift results. It was found that, with the increase in the energy (the reduction in the dot size), the diamagnetic coefficient first rises quickly and then saturates at around 21 $\mu eV/T^2$. Based on a simple calculation model, this unusual tendency is attributed to the electrons gradually spilling out of the quantum dot to the wetting layer as the dots get smaller. This delocalization effect is enhanced in this material system due to the tensile strain relaxation within the dots, which raises the conduction band edge over that in the wetting layer.
 [doi:10.1063/1.3520669]

I. INTRODUCTION

Type-II self-assembled quantum dots (SAQDs) have attracted considerable interest for the application of carrier storage,[1] spin storage device,[2] and the exhibition of optical Aharnov–Bohm effect in magnetic fields[3,4] owing to the spatial separation between the electrons and holes. To date, most SAQD structures are fabricated by the natural compressive strain due to the lattice mismatch between different materials. Recently, the QD formation driven by tensile strain in the GaAs/GaSb type-II heterostructure with GaAs dots in GaSb matrix has been reported. The mid-IR optical response of the type-II transition is able to be extended to a longer wavelength because of the band gap shrinkage induced by tensile strain.[5]

In this work, we studied the magneto-optical properties of GaAs QDs in GaSb matrix. Because of the type-II band alignment, electrons are localized in GaAs QDs while holes are confined to the GaSb region next to GaAs by the Coulomb interaction. As the size of the QDs is changed, an unusual correlation was found between the diamagnetic coefficient and the emission energy. We attributed this phenomenon to the weak localization of electrons within the small-sized QDs in the tensily strained system. A theoretical model was proposed and the calculated results agree very well with the experimental findings.

II. EXPERIMENT

The GaAs QDs were grown on n+GaSb (001) substrates by a Veeco Gen-II molecular beam epitaxy (MBE) system with valve cracker sources of Sb_2 and As_2 molecules. Three samples with different amount of deposited GaAs for QD formation were prepared. They were: (1) sample A with 2.0 monolayers (ML) of GaAs, (2) sample B with 2.3 ML of GaAs, and (3) sample C with 2.5 ML of GaAs. The growth temperature was 500 °C, the V/III beam equivalent pressure ratio for GaAs was 3, and the growth rate was 0.1 ML/s, which was taken from that of 0.086 ML/s for GaAs homoepitaxial growth calibrated using reflection high-energy electron diffraction oscillation. To improve the GaAs QD uniformity, the migration enhanced epitaxy (MEE) technique was used for the QD growth. A 2 s growth interruption was used after every 0.5 ML of GaAs was deposited. The GaAs QD layer was embedded in a 100 nm GaSb matrix, which was sandwiched with two 20 nm $Al_{0.3}Ga_{0.7}Sb$ barriers. These barriers were used to confine carriers and thus improve the PL intensity.

The embedded GaAs QDs were characterized by a transmission electron microscope (TEM) (JEOL 2010F TEM) operated at 200 keV. The TEM specimens were prepared using cross-section and plan-view thinning in a Gatan 691 ion mill. Conventional photoluminescence and magneto-PL measurement were performed at 1.4 K with a 14 T superconducting magnet. The excitation source was a 532 nm Nd:yttrium aluminum garnet (YAG) laser coupled through an optical fiber with a focusing lens. The PL signal was collected with a fiber bundle, dispersed by a 500 mm monochromator, and detected by a wavelength-extended InGaAsSb detector.

The embedded GaAs QDs were characterized by a TEM (JEOL 2010F TEM) operated at 200 keV. The TEM specimens were prepared using cross-section and plan-view thinning in a Gatan 691 ion mill. Magneto-PL measurement was performed at 1.4 K in high magnetic fields up to 14 T in a Faraday configuration. The excitation source was a 532 nm

[a)]Electronic mail: dajin6@yahoo.com.tw.

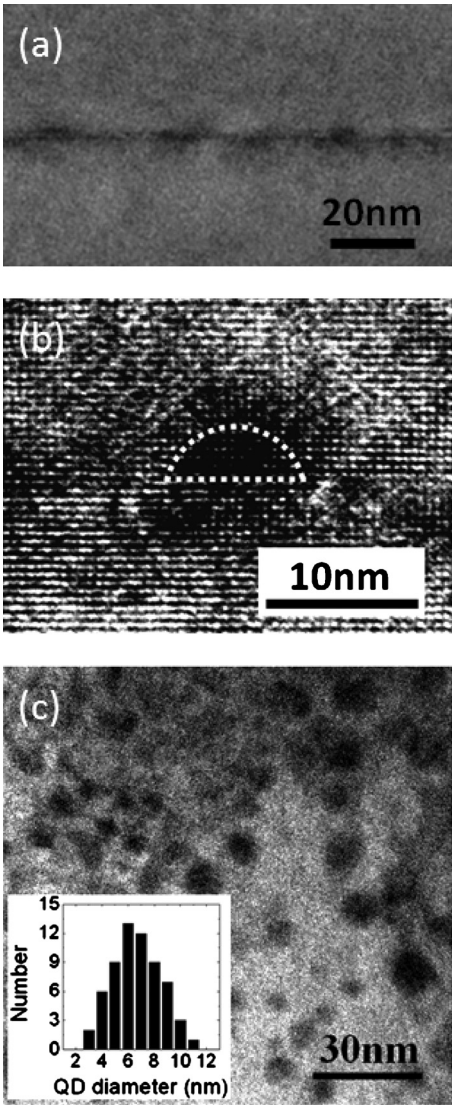

FIG. 1. Cross-section (a) TEM and (b) HRTEM images of GaAs QDs in GaSb matrix along the $[010]_{GaSb}$ zone axis. We estimated the average width of QDs as 6.7 nm from (c) the plan-view image taken along $[001]_{GaSb}$ axis. The inset shows the distribution of the QD diameter.

Nd:YAG laser coupled through an optical fiber with a focusing lens. The PL signal was collected with a fiber bundle, dispersed by a 500 mm monochromator, and detected by a wavelength-extended InGaAsSb detector.

III. RESULTS AND DISCUSSION

A. Structural properties

The TEM samples were taken from sample A. The cross-sectional and plan-view images are presented in Figs. 1(a)–1(c), respectively. The dark areas arising from strain contrast revealed small-sized QDs. From the images, the QDs were estimated to have an aspect ratio of 2.5:1 (width of 9 nm and height of 3.6 nm) and the areal density of 3×10^{11} cm^{-2}. The size distribution was shown in the inset of Fig. 1(c). The average base width of the dots was 6.7 nm, which is smaller than that of the conventional compressively strained QDs.[6,7] Because of the small dot size, the confined electron states were expected to be close to that of the wetting layer (WL).

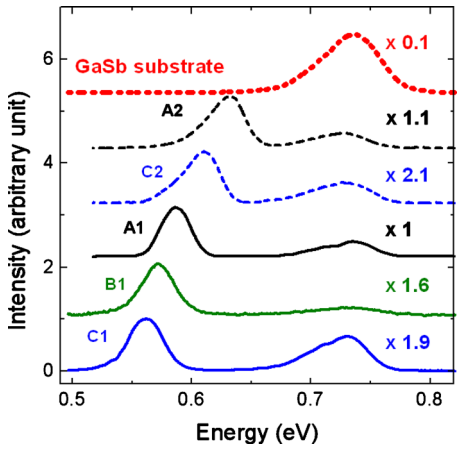

FIG. 2. (Color online) PL spectra of the three samples and the GaSb substrate. The solid lines, A1, B1, and C1, are from the central area of these samples. The dashed lines, A2 and C2, are from the samples' edge.

B. Conventional PL and the excitation power dependence

Figure 2 shows the PL spectra of our samples along with that of the GaSb substrate taken as a reference. A broad emission centered at 0.73 eV is seen for all samples (even for the reference sample, the red dotted line). Since this emission energy is below the GaSb band gap of 0.812 eV, it is hence attributed to the impurities or defects within the GaSb substrate. The low energy emissions labeled as A1, B1, and C1 are from the central area of these samples and are attributed to the GaAs QDs. The lowest PL peak energy of 0.564 eV ($\sim$2.2 μm) is from the largest QDs of sample C1 as a result of the largest amount of deposited GaAs. The PL intensity of C1 is almost half that of A1 due to the more separated electrons and holes for larger type-II dots. Note that the full width at half maximum (FWHM) is 33 meV here, which is smaller than that in Ref. 5 of around 50 meV. The small FWHM indicates that a more uniform QD size distribution, especially in height, is achieved probably by the MEE method.

The dashed lines (labeled as A2 and C2) show the PL from the samples' edge, where the growth temperature is about 20 °C lower than that of the central area. The QDs formed in the edge are therefore expected to be smaller. These emission peaks have the asymmetric shape with a low energy band tail, which may be attributed to the QDs with less uniform size distribution due to lower growth temperature. However, in Sec. III C, the magneto-PL measurement which probes the in-plane spatial extent of the carrier wave function reveals that the origins of these two peaks are from the GaAs WLs. The energy tail has also been found in other Sb-contained or N-contained quantum wells (QWs) and WLs,[8–12] and is attributed to the localized states from alloy composition fluctuation, well thickness irregularity, and other crystal imperfections.[8]

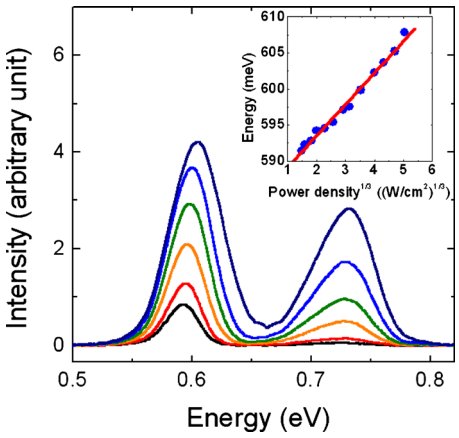

FIG. 3. (Color online) Representative power-dependent PL spectra from A1. The excitation power density is varied from 4 to 80 W/cm^2. The inset shows the emission peak energy of GaAs QDs plotted against the cubic root of the excitation power density.

As the excitation power increases, all the emission peaks exhibit energy blueshifts, except that from the GaSb substrate. A representative series of power-dependent PL spectra from sample A1 are illustrated in Fig. 3. The blueshift is in proportional to the 1/3 power of excitation power as seen in the inset, which is a clear signature of type-II heterostructure. The spatial separation between electrons and holes in the GaAs/GaSb heterostructures leads to the long carrier recombination time and hence the dramatically increased carrier density with the excitation power. The accumulated electrons confined inside the QDs or WLs fill the electron high energy states and induce a triangular potential well in the GaSb next to GaAs and hence raise the energies of holes. These so-called state filling and band bending effects give rise to the energy blueshifts.[13,14]

C. Magneto-PL

The PL spectra of GaAs QDs have been measured as a function of the magnetic field in a Faraday configuration; those from A1 and C1 are shown in Fig. 4. The PL intensity is enhanced with magnetic field (by about 40% at 14 T) due to the additional confinement of carriers from the magnetic field. The blueshift in energy peak, the diamagnetic shift, has a quadratic dependence on magnetic field. The diamagnetic shift can be well described by the following simple equation when the field is relatively low

$$\Delta E = \beta B^2 = \frac{e^2\langle\rho_e\rangle^2 B^2}{8m_e} + \frac{e^2\langle\rho_h\rangle^2 B^2}{8m_h},$$

where β is the diamagnetic coefficient, ρ_e (ρ_h) is the radius of the electron (hole) wave function projected on the plane perpendicular to the magnetic field, and m_e (m_h) is the electron (hole) effective mass. The diamagnetic coefficient of the larger QDs from C1 is 7.6 μeV/T^2. Interestingly, the smaller QDs from A1 show a considerably larger diamagnetic coefficient of 17.3 μeV/T^2, which is more than double that of the larger QDs. This result suggests that the carrier wave function of the smaller QDs is more extended than that of the larger QDs. This behavior is unexpected for regular sized QDs because the wave functions are generally restricted to a smaller area when the dots get smaller.[15] It should be mentioned that the excitation power is kept very low at 1 W/cm^2 for the magneto-PL study to reduce the state filling and band bending effects.

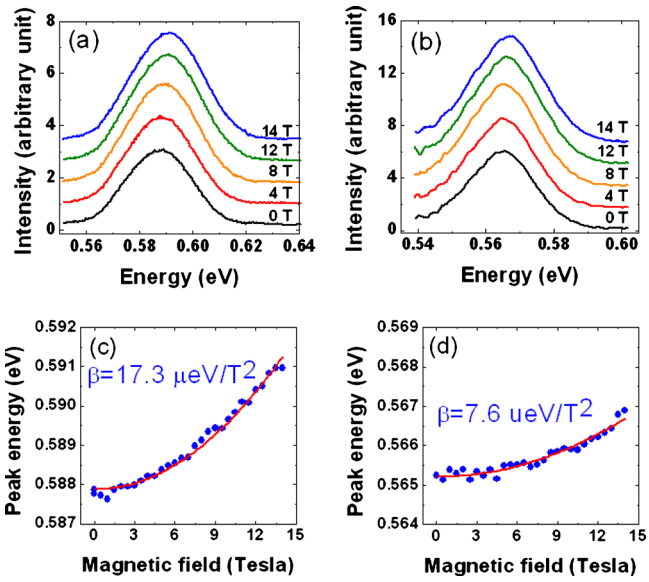

FIG. 4. (Color online) The magneto-PL spectra from (a) A1 and (b) C1. The emission peak energy is fitted to the square of the magnetic field for (c) A1 and (d) C1.

We have performed the measurements on various locations of the three samples to study the dependence of the diamagnetic coefficient as a function of the emission energy. The result is plotted in Fig. 5. The solid symbols represent the emission peaks with symmetric shapes which are assigned as QD optical transitions. On the other hand, the open symbols represent the asymmetric emissions with low energy band tails. The diamagnetic coefficient first increases quickly with the emission energy for the QD emissions and then saturates around 21 μeV/T^2 for those asymmetric emissions. This saturated stable diamagnetic coefficient indicates that the in-plane spatial extent of the carrier wave function is almost independent of the confinement potential. We there-

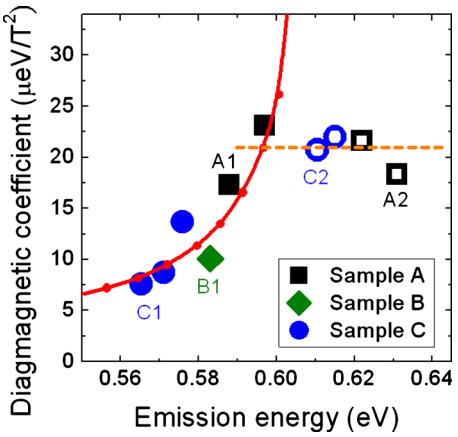

FIG. 5. (Color online) The diamagnetic coefficient against the emission energy of sample A (black squares), sample B (green diamonds), and sample C (blue circles). The solid (open) symbols represent the emissions with symmetric (asymmetric) PL shapes. The scalculation results are also plotted here as the red solid line.

fore convincingly attribute those asymmetric emissions as type-II WL emissions. The diamagnetic shift in WL in a Faraday configuration depends on the electron-hole separation. For type-I QWs with infinite barriers, the electron-hole separation decreases as the well thickness is reduced due to the enhancement of their Coulomb interaction.[16] However, the spatially separated electron-hole pair of type-II structure causes the lateral separation less sensitive to the well thickness.

Now we turn to the QD emissions. We attribute the increase in the diamagnetic shift with emission energy to two specific properties of the GaAs/GaSb QDs: the tensily strained system and the small QD dimension. Unlike the common compressively strained system, where the partial strain relaxation and the larger height (compared to WL) make the QD energy much lower than that of the WLs, the tensile-strain relaxation within the GaAs/GaSb QDs substantially raises the band gap energy and compensates the effect of the larger height of the QD. The electron ground state of the QDs hence gets close to or even goes beyond that of the WL, which is fully strained, as the QDs get smaller. As a consequence, the electrons spread out of the QD to the WL, therefore causing an increased diamagnetic coefficient, which eventually saturates at that of the WL.

D. Simulation

We have calculated the electron wave functions using one-band effective mass Hamiltonian. The diameter of the lens-shaped QDs with an aspect ratio of 2.5:1 is varied from 4 nm to 28 nm. A WL of 1 nm thickness is placed below the QD. The composition of the QD, the WL, and the matrix is taken as $GaAs_{0.8}Sb_{0.2}$, $GaAs_{0.45}Sb_{0.55}$, and $GaAs_{0.1}Sb_{0.9}$ to account for partial intermixing of As and Sb atoms during growth.[5,17] Besides, the WL and the pseudomorphically grown matrix are taken to be fully strained matching the lattice constant of GaSb,[5] but the QD is assumed to be 25% strain relaxed. The band diagram of a QD and the adjacent WL under full strain (dotted line) and with the partially relaxed strain in the QD for light-hole state (solid line) and the heavy-hole state (dashed line) is illustrated in the inset of Fig. 6(a). The parameters used in the calculation are taken from Ref. 18. Due to the small dot size and large conduction band offset (480 meV), the electrons are confined inside the dot at a high quantization energy. The effective mass is therefore taken as high as 0.08 m_0 owing to the conduction band nonparabolicity.[19] The diamagnetic response can be further calculated by superimposing a magnetic confining potential to the Hamiltonian and then fitted to $\Delta E = \beta B^2$ to find the electron-contributed diamagnetic coefficient.

Holes are confined to the Ga(As)Sb region near the QD in this type-II system due to the Coulomb attraction to electrons. However, the complicated strain distribution near the QD (with compressive strain in the vicinity of the dot and tensile strain elsewhere) is expected to distort the potential profile for holes and mix the light hole and heavy-hole states. To simplify the calculation, we assume that the hole wave function has the same radius as that of the electron wave function, and the hole effective mass is taken to be 0.23 m_0,

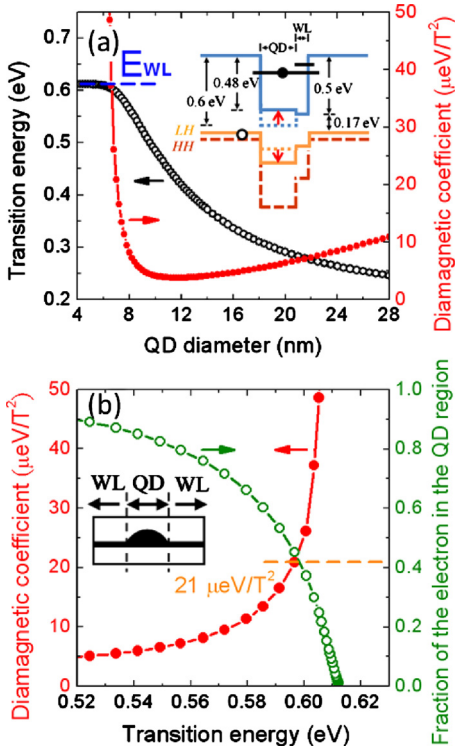

FIG. 6. (Color online) (a) The calculated transition energy and the corresponding diamagnetic coefficient with the diameter of the QD. The inset shows the band diagram of a QD and the adjacent WL under full strain (dotted line) and with the 20% relaxed strain in the QD for the light-hole state (solid line) and for heavy-hole one (dashed line). (b) The diamagnetic coefficient and the fraction of the electron localized in the QD region against the transition energy. The regions of QD and WL are defined as illustrated in the inset.

which is the average of the heavy hole and light hole effective mass of GaSb. Consequently, the hole-contributed diamagnetic coefficient is about 1/3 of the electron-contributed one.

The calculated transition energy and the corresponding diamagnetic coefficient are plotted in Fig. 6(a) against the diameter of the QD. When the diameter of the QD is larger than 11.5 nm, the diamagnetic coefficient increases with the QD diameter as expected for regular sized QDs. However, as the QD diameter gets smaller than 11.5 nm, the wave function starts to spread into the WL, the transition energy is approaching to the WL emission energy, and the corresponding diamagnetic response is significantly enhanced. Since the GaAs QDs in GaSb matrix are usually very small[5] and all the dots used in this work are smaller than 11 nm, the rising trend of the diamagnetic coefficient is observed as the QDs get smaller. To compare with the experimental data, the calculated diamagnetic coefficient is plotted (for the small dots) as a function of the transition energy as the red solid lines in Figs. 5 and 6(b). It agrees very well with the experimental data until the rising diamagnetic coefficient exceeds that of the WL at 21 $\mu eV/T^2$, the orange dashed line. In this situation, the electron-hole Coulomb interaction starts to play an important role, and this simplified model becomes invalid. In Fig. 6(b), by defining the QD and WL region as the inset, we calculate the fraction of the electron localized in the QD and plot it as the green line. In the calculation, the electron wave

function dramatically spreads out of the QD to the WL as the diamagnetic coefficient gets larger than 21 $\mu eV/T^2$, the experimental value of the WL.

IV. CONCLUSIONS

In summary, type-II tensily strained GaAs QDs in GaSb with mid-IR emission up to 2.2 μm were grown by MBE and studied by magneto-PL for the first time. By comparing several samples with different GaAs deposition amount, the diamagnetic coefficient was found to rise quickly from 7.6 $\mu eV/T^2$ to a saturated value of around 21 $\mu eV/T^2$ with the emission energy. This unusual behavior is due to the spreading of the electron wave function from the QD to the WL as the dots get smaller. A theoretical calculation of the diamagnetic shift in this type-II QD system considering the strain effect is performed and the results agree with the experimental finding.

ACKNOWLEDGMENTS

We acknowledge the support from the National Science Council under Contract Nos. NSC96-2221-E-009-211-MY3 and NSC98-2120-M-009-002, Center for Nano Science and Technology of National Chiao Tung University, National Nano Device Laboratories, and "Aim for the Top University Plan" of the National Chiao Tung University and Ministry of Education,Taiwan, R.O.C.

[1]M. Geller, C. Kapteyn, L. Müller-Kirsch, R. Heitz, and D. Bimberg, Appl. Phys. Lett. **82**, 2706 (2003).
[2]H. Gotoh, H. Ando, H. Kamada, A. Chavez-Pirson, and J. Temmyo, Appl. Phys. Lett. **72**, 1341 (1998).
[3]E. Ribeiro, A. O. Govorov, W. Carvalho, Jr., and G. Medeiros-Ribeiro, Phys. Rev. Lett. **92**, 126402 (2004).
[4]I. R. Sellers, V. R. Whiteside, I. L. Kuskovsky, A. O. Govorov, and B. D. McCombe, Phys. Rev. Lett. **100**, 136405 (2008).
[5]A. A. Toropov, O. G. Lyublinskaya, B. Ya. Meltser, V. A. Solov'ev, A. A. Sitnikova, M. O. Nestoklon, O. V. Rykhova, S. V. Ivanov, K. Thonke, and R. Sauer, Phys. Rev. B **70**, 205314 (2004).
[6]H. Saito, K. Nishi, and S. Sugou, Appl. Phys. Lett. **74**, 1224 (1999).
[7]F. Hatami, N. N. Ledentsov, M. Grundmann, J. Böhrer, F. Heinrichsdorff, M. Beer, D. Bimberg, S. S. Ruvimov, P. Werner, U. Gösele, J. Heydenreich, U. Richter, S. V. Ivanov, B. Ya. Meltser, P. S. Kop'ev, and Zh. I. Alferov, Appl. Phys. Lett. **67**, 656 (1995).
[8]M. Dinu, J. E. Cunningham, F. Quochi, and J. Shah, J. Appl. Phys. **94**, 1506 (2003).
[9]M. C. Lo, S. J. Huang, C. P. Lee, S. D. Lin, and S. T. Yen, Appl. Phys. Lett. **90**, 243102 (2007).
[10]Y.-H. Cho, T. J. Schmidt, S. Bidnyk, G. H. Gainer, J. J. Song, S. Keller, U. K. Mishra, and S. P. DenBaars, Phys. Rev. B **61**, 7571 (2000).
[11]J. Bai, T. Wang, and S. Sakai, J. Appl. Phys. **88**, 4729 (2000).
[12]F. Ishikawa, Á. Guzmán, O. Brandt, A. Trampert, and K. H. Ploog, J. Appl. Phys. **104**, 113502 (2008).
[13]W. H. Chang, Y. A. Liao, W. T. Hsu, M. C. Lee, P. C. Chiu, and J. I. Chyi, Appl. Phys. Lett. **93**, 033107 (2008).
[14]N. N. Ledentsov, J. Böhrer, M. Beer, F. Heinrichsdorff, M. Grundmann, D. Bimberg, S. V. Ivanov, B. Ya. Meltser, S. V. Shaposhnikov, I. N. Yassievich, N. N. Faleev, P. S. Kop'ev, and Zh. I. Alferov, Phys. Rev. B **52**, 14058 (1995).
[15]M. Sugisaki, H. W. Ren, S. V. Nair, K. Nishi, and Y. Masumoto, Phys. Rev. B **66**, 235309 (2002).
[16]S. N. Walck and T. L. Reinecke, Phys. Rev. B **57**, 9088 (1998).
[17]R. Timm, H. Eisele, A. Lenz, S. K. Becker, J. Grabowski, T.-Y. Kim, L. Müller-Kirsch, K. Pötschke, U. W. Pohl, D. Bimberg, and M. Dähne, Appl. Phys. Lett. **85**, 5890 (2004).
[18]I. Vurgaftman, J. R. Meyer, and L. R. Ram-Mohan, J. Appl. Phys. **89**, 5815 (2001).
[19]D. F. Nelson, R. C. Miller, and A. A. Kleinman, Phys. Rev. B **35**, 7770 (1987).